Biol. Cybern. 52, 101–107 (1985)

Biological Cybernetics

Multiplication and Refractoriness in the Cat's Retinal-Ganglion-Cell Discharge at Low Light Levels

B. E. A. Saleh[1] and M. C. Teich[2]

1 University of Wisconsin, Madison, WI 53706, USA
2 Columbia University, New York, NY 10027, USA

Abstract. Measurements of the pulse-interval distribution and pulse-number distribution for cat retinal ganglion cells in darkness and light have been carried out by Barlow, Levick, and Yoon. The experimental results for an on-center brisk-sustained cell are in accord with a mathematical model incorporating four features: Poisson quantum fluctuations, additive dark noise, multiplication noise (random multiple neural spikes per absorbed quantum), and refractoriness. The data cannot be properly explained by a model lacking any one of these features. Parameters extracted from the model are in good agreement with physiological values.

1 Introduction

There are many processes in the visual system whose explanation invokes Poisson quantum fluctuations. The simplest examples, perhaps, are the the detection of low-level light (e.g., the Hecht-Shlaer-Pirenne experiment [1]) and the statistics of spike trains [2] recorded from at least some retinal ganglion cells [3]. It is now well known, however, that the Poisson hypothesis by itself cannot provide a satisfactory explanation for either of these processes. The principal remedy that has been applied in attempts to improve the capabilities of this simple model is the introduction of additive Poisson noise [4, 5]. This is a sensible addition because it is known that there are spontaneous firings in the visual system. It turns out that the assumptions of Poisson quantum fluctuations together with additive Poisson noise can indeed provide a satisfactory fit for certain measures of the neural point process, e.g., the receiver-operating characteristic (ROC) [5]. However, the level of noise required to be added to satisfy the experimental data is found to vary with the stimulus level. As a result, multiplicative noise in neural firings has been suggested as another important process in visual information processing [2, 6–8]. According to this mechanism, every detected quantum may result in several nerve spikes (the number may be random and the average may be greater than 1). If the number of nerve spikes *per detected quantum* is Poisson distributed, the Neyman Type-A distribution (NTA) results [7]. This distribution has the property that the count variance is propertional to, but greater than, the count mean. This is consistent with experiment and can be used to explain the deviation of the pulse-interval distribution (PID) from the exponential form associated with a Poisson process [8, 9]. However, multiplication noise alone cannot explain the depressed probability at short time intervals exhibited by the PID. Refractoriness (dead time) is the obvious explanation for this; unfortunately, however, incorporating dead time in the pulse-number distribution (PND) turns out to be somewhat complex from a mathematical point of view.

In a study carried out in 1981, we showed [8] that the PID of a spontaneously firing brisk-sustained on-center cat retinal ganglion cell, measured by Barlow, Levick, and Yoon (BLY) [2], could be properly fit when additive and multiplicative noise, as well as Poisson quantum fluctuations and refractoriness, were included in the mathematical model. Barlow, Levick, and Yoon have provided us with experimental PND data for this same cell. It is the purpose of this paper to show that this mathematical model also provides good fits to the PNDs. We believe that this is the simplest model than can satisfactorily account for the PID, the PNDs, and the ROCs for a retinal ganglion cell both in darkness and in light. Barlow, Levick, and Yoon measured PNDs in response to brief flashes of light for several cells. A PID histogram for the time between successive spikes in unit BLF-1 (an on-center brisk-sustained unit) was recorded in darkness. They con-

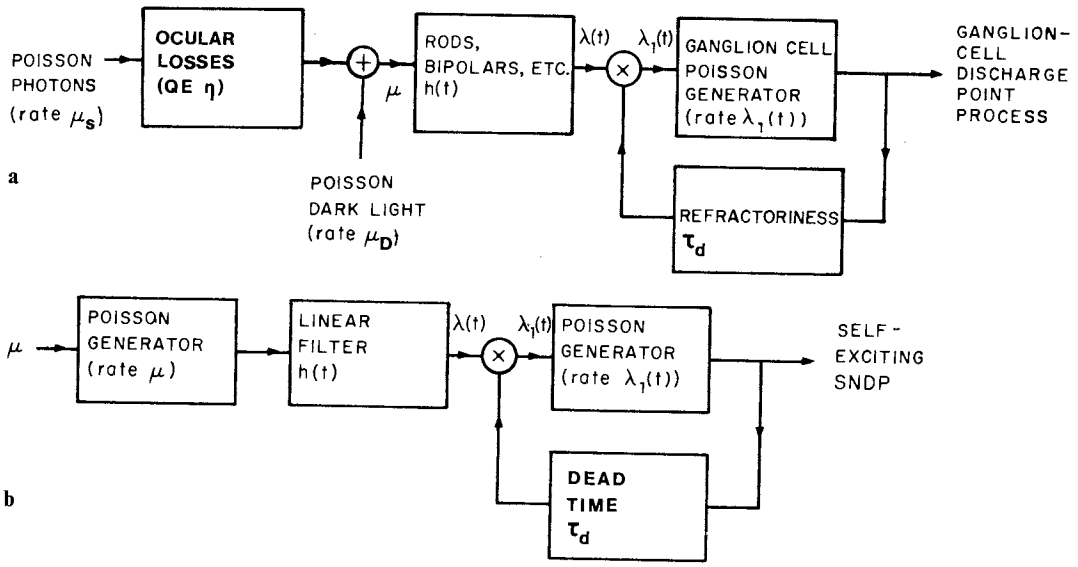

Fig. 1. **a** Model for the generation of the neural discharge point process for an on-center brisk-sustained retinal ganglion cell. **b** Schematic representation of the shot-noise-driven doubly stochastic Poisson point process (SNDP) with dead time (self-excitation). The identity is evident

cluded from this study that dark-light events can cause multiple impulses at the ganglion cell, and that dark-light events behave like quantal absorptions in this respect. They pointed out that the statistical properties of the maintained discharge are similar in darkness and for light-evoked responses, indicating that the discharge behaves as though it results from random unitary events in the receptors, each causing several impulses. They also observed that the deficit of short time intervals in the PID may be the result of relative refractoriness. A related study carried out at various weak levels of light adaptation produced experimental results consistent with the earlier study [5].

Since that time, Baylor and Yau and their collaborators [10–13] demonstrated that the current pulses in the vertebrate rod outer segment take a Poisson form. This is true both in darkness and at low light levels, and apparently reflects the Poisson form of spontaneous and photon-induced rhodopsin isomerizations, respectively. The quantum fluctuations, it seems, are augmented by Poisson dark events and both are carried forward to the rod response at the outer segment.

Based on the results of the Barlow, Levick, and Yoon and Baylor studies, we constructed a model (see Fig. 1a) for the generation of the neural-discharge point process in an on-center cell [8]. Poisson photons incident on the cornea (rate μ_S) pass through the ocular medium to excite rods (quantum efficiency η). Combined with Poisson dark light (rate μ_D), this produces an overall Poisson rate $\mu=\mu_S+\mu_D$ which excites a complex network of rods, bipolars, and other cells, that is represented in terms of a linear-filter impulse response function $h(t)$ [14]. The result is a shot-noise process [9] denoted by $\lambda(t)$ which, after a modification to be discussed below, provides the time-varying driving rate $\lambda_1(t)$ for the ganglion cell. Our model assumes that the ganglion cell would, in the absence of fluctuations of $\lambda_1(t)$, produce a pure Poisson discharge. In the presence of fluctuations, the discharge will follow a doubly-stochastic Poisson process (DSPP) [9]. A simpler way of understanding this is in terms of the equivalent Neyman-Scott cluster process [9] in which a *single* incident photon generates a randomly delayed Poisson-distributed cluster of neural spikes. These multiple firings per incident quantum (multiplication) could arise from a very strong rod response to a photon absorption or, as Barlow, Levick, and Yoon suggest, from multiple pathways in the retina between rod and ganglion cell.

The modification mentioned above is refractoriness which, when a neural spike is generated, depresses the excitability of the cell. The recovery of the neuron is represented in terms of a refractoriness period τ_d that sets the input (and therefore the output) of the ganglion cell at zero for a time τ_d following the registration of a nerve spike. The output of the system represents the ganglion-cell discharge point process.

In Fig. 1b we present a diagram for the shot-noise-driven doubly stochastic Poisson point process (SNDP) with dead time (self-excitation) that we earlier proposed [8] as a representation of the ganglion-cell discharge point process and analyzed mathematically for the PID (for ease of calculation we now treat the refractoriness as absolute rather than as relative, as was allowed in [8]). The identity between Fig. 1a and b is evident.

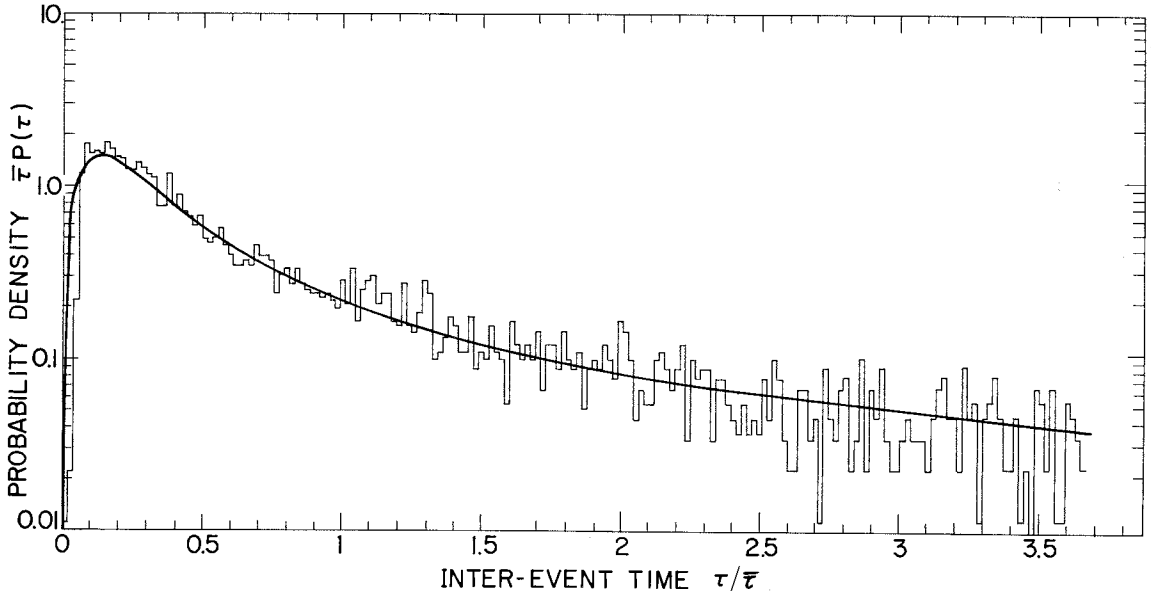

Fig. 2. Maintained discharge interspike-interval histogram recorded by Barlow et al. [2] for a dark-adapted on-center brisk-sustained cat retinal ganglion cell in darkness (unit BLF-1). The mean time interval is 54.25 ms. Scales are normalized such that $\langle\tau\rangle = 1$. Theoretical fit (solid curve) is based on an exponential shot-noise filter impulse response function with normalized time constant $\tau_p/\langle\tau\rangle = 0.5$ ($\tau_p \approx 27$ ms), an exponential relative-refractoriness recovery function with normalized time constant $\tau_d/\langle\tau\rangle = 0.1$ ($\tau_d \approx 5.4$ ms), and a multiplication parameter $\alpha \approx 2$. (After Teich and Saleh [8])

2 Dark Pulse-Interval Distribution

The experimental maintained-discharge interspike-interval histogram for unit BLF-1 is presented in Fig. 2 with a bin width of 1 ms. The data in Fig. 2 differ slightly from those in Fig. 5A in the Barlow, Levick, and Yoon paper, where pairs of adjacent channels were combined before plotting, so that the bin width there is 2 ms [15]. The two presentations also differ (insubstantially) in that the histogram in Fig. 2 has been normalized to the experimental mean interevent time (54.25 ms). This value will differ only slightly from the mean interevent time in the absence of self-excitation.

The theoretical interevent-time density function for exponential shot-noise pulses and relative refractoriness in the form of gradual exponential recovery is presented in Eqs. (28)–(35) of [8]. After some experience with a parametric study, a good fit was obtained with relative ease (solid curve). This led to the following values for the three parameters for unit BLF-1 in darkness: a relative-refractoriness time $\tau_{rd} \approx 5.4$ ms, a shot-noise decay time $\tau_p \approx 27$ ms, and a multiplication parameter $\alpha \approx 2$. It is, perhaps, worth pointing out that the maintained discharge recorded from the lobula complex of the blowfly exhibits similar behavior [16].

3 Dark Pulse-Number Distribution

We now proceed to demonstrate that the count mean and variance of the PND for the dark discharge of this same unit are consistent with the model presented in Fig. 1. Indeed, the same set of parameters (with one modification to be explained below) provides agreement between theory and experiment for both the PID and the PND. This is an important observation since the two distributions reflect different properties of the underlying neural point process [17]. The agreement strengthens the appeal of the model.

To carry out our analysis, we make use of theoretical results for the dead-time-modified SNDP [18]. These results include expressions for the count mean and variance for fixed nonparalyzable dead time (rather than the more general relative refractoriness or gradual recovery) and for a rectangular (rather than exponential) impulse-response function of time constant τ_p and area α. Nevertheless, the theory should apply quite well to the problem at hand because the PND effectively averages the recovery time function when T is sufficiently large [19] and the behavior of the SNDP is only weakly dependent on the form of $h(t)$ [9].

The count mean and variance are expressed in terms of modification factors ε_m and ε_v. The quantity ε_m is the ratio of the means with and without dead-time modification whereas ε_v is the ratio of the variances with and without dead-time modification. The mean of the shot-noise-driven Poisson process (SNDP) in the absence of dead time is $\langle n\rangle = \mu\alpha T$, where T is the counting time. The variance of the SNDP in the absence of dead time is $\langle(\Delta n)^2\rangle = \mu\alpha T(1 + \alpha/\mathscr{M})$, where

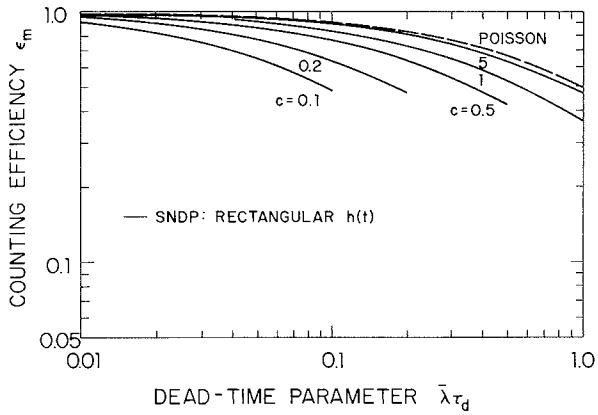

Fig. 3. Counting efficiency for the mean, $\varepsilon_m = \mathrm{E}(n)/\mu\alpha T$ versus $\bar{\lambda}\tau_d = \mu\alpha\tau_d$, where $\mu\alpha$ is the average driving rate, τ_d is the dead time, and T is the counting time. Curves are for a homogeneous Poisson process (dashed curve) and for a shot-noise-driven Poisson process (SNDP) with rectangular impulse response function (solid curves). The dependence of the counting efficiency on the parameter $c = \mu\tau_p$ is indicated. The curves extend only up to their range of validity for $\alpha = 5$. (After Saleh et al. [18])

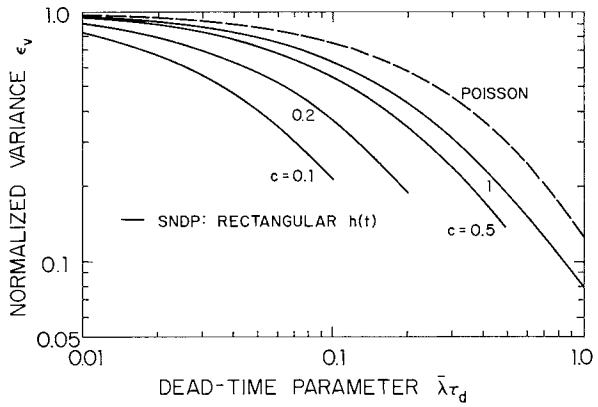

Fig. 4. Normalized variance (ratio of dead-time-modified variance to unmodified variance) ε_v versus $\mu\alpha\tau_d$, where $\mu\alpha$ is the average driving rate and τ_d is the dead time. Curves are for a homogeneous Poisson process (dashed curve) and for a shot-noise-driven Poisson process (SNDP) with rectangular impulse response function (solid curves). The dependence of the normalized variance on the parameter $c = \mu\tau_p$ is indicated. Curves are shown for $\alpha = 5$ and $\Gamma = 10$, but are essentially independent of these parameters. The curves extend only up to their range of validity for $\alpha = 5$. The dependence of ε_v is seen to be similar to the dependence of ε_m presented in Fig. 3. (After Saleh et al. [18])

$\mathscr{M}$ is a degrees-of-freedom parameter that depends on the ratio $\Gamma = T/\tau_p$. For $\Gamma \gg 1$ we have $\mathscr{M} = 1$ and the NTA distribution results. Subject to some restrictions, expressions for the counting efficiency ε_m and the normalized variance ε_v (as a function of the dead-time parameter $\bar{\lambda}\tau_d = \mu\alpha\tau_d$) are available for an equilibrium dead-time counter with arbitrary counting time T and $\tau_d \ll \tau_p$ [18]. Although the mathematical results are somewhat complex, the behavior of ε_m and ε_v is rather simple and has been illustrated graphically in [18].

In Fig. 3, we present a plot of the theoretical SNDP counting efficiency ε_m, as a function of the dead-time parameter $\mu\alpha\tau_d$. The quantity ε_m depends only on $\mu\alpha\tau_d$ (the abscissa) and on $c = \mu\tau_p$ which is the number of primary events per correlation time (this is sometimes called the degeneracy parameter). The dependence on c is shown parametrically. In Fig. 4, we show the behavior of the theoretical normalized count variance ε_v as a function of $\mu\alpha\tau_d$. This quantity essentially depends only on $\mu\alpha\tau_d$ and $c = \mu\tau_p$, as does ε_m. In actuality, ε_v also depends on α and on $\Gamma = T/\tau_p$, but this dependence is very slight and may be disregarded to good approximation [18]. All curves in Figs. 3 and 4 are shown only up to their range of validity for $\alpha = 5$. The dashed curves are the limiting case of a dead-time-modified homogeneous Poisson point process. The physical significance of the variations in ε_m and ε_v is discussed in [18].

The set of parameters that was initially used to fit the PID for unit BLF-1 in the dark was $\tau_{rd} \approx 5.4$ ms, $\tau_p \approx 27$ ms, and $\alpha \approx 2$. The value of τ_{rd} obtained for the fit presented in [8] and Fig. 2 was based on relative refractoriness. However, as we have pointed out, formulas for the PND mean and variance could be readily derived only for a fixed dead time τ_d. To account for this difference we found it necessary to set τ_d to a value of 1.7 ms. Using this value, together with a counting time $T = 0.2$ s, a fit to the dark PND measured by Barlow, Levick, and Yoon is obtained with a dark-rate $\mu_D = 16.5\,\mathrm{s}^{-1}$. With these parameters, the model results in a theoretical count mean $\mathrm{E}(n) = 5.61$ and a theoretical count variance $\mathrm{Var}(n) = 12.86$. These are in good accord with the experimental values of 5.65 and 12.81 for the experimental mean and variance, respectively.

4 PND in the Presence of Light

In Fig. 5 we present values (open circles) for the experimental count variance $\mathrm{Var}_{\mathrm{exp}}(n)$ versus the experimental count mean $\mathrm{E}_{\mathrm{exp}}(n)$ obtained by Barlow, Levick, and Yoon in a counting time $T = 0.2$ s for unit BLF-1. The data points represent responses to flashes of light of varying energy (ranging from 0 to 100 quanta/flash). Each data point corresponds to 100 trials.

The solid curve is the theoretical result associated with the model shown in Fig. 1. It has been fit to the data as follows: Four parameters ($\tau_d = 1.7$ ms, $\tau_p = 27$ ms, $\alpha = 2$, and $\mu_D = 16.5\,\mathrm{s}^{-1}$) were a priori selected on the basis of our experience in fitting the PID and the dark PND mean and variance. Then one data point in the presence of light [$\mathrm{E}_{\mathrm{exp}}(n) = 7.41$,

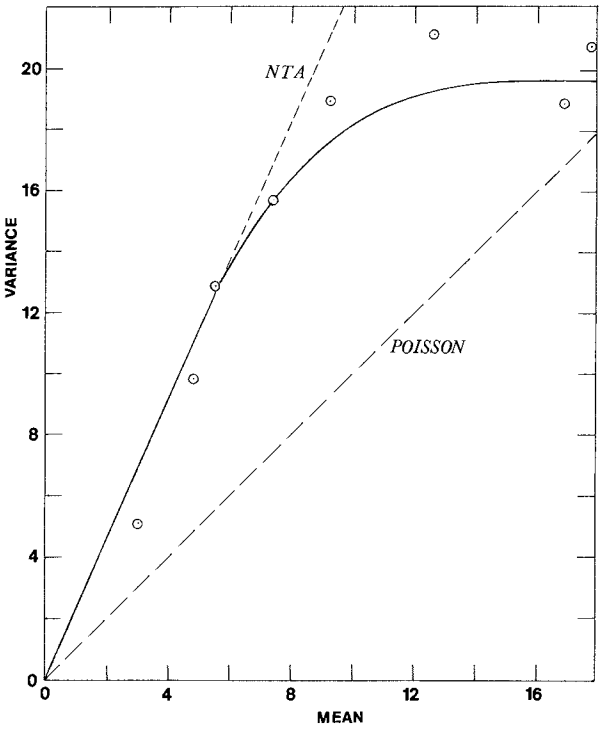

Fig. 5. Count variance versus count mean for on-center brisk-sustained retinal ganglion cell BLF-1. Open circles represent experimental data points collected by Barlow, Levick, and Yoon [2]. Solid curve is the theory developed here. Dashed lines represent the Poisson and the best-fitting Neyman Type-A (NTA) distributions

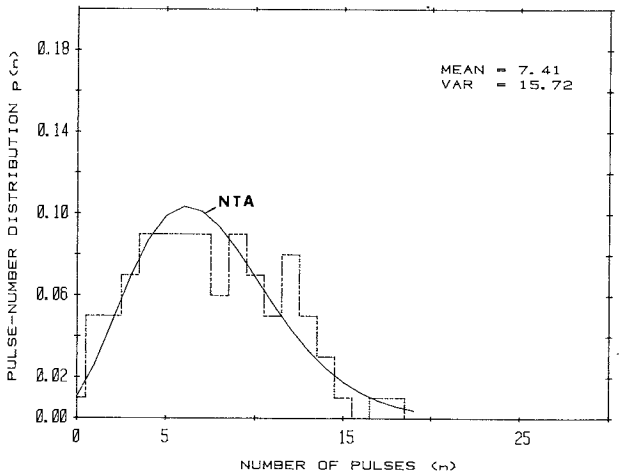

Fig. 6. Pulse-number histogram for Unit BLF-1 in response to a 10-ms flash of light ($T=0.2$ s). The mean count $E_{exp}(n)=7.41$ and $Var_{exp}(n)=15.72$. Theoretical fit (solid curve) is the Neyman Type-A (NTA) distribution with these parameters

$Var_{exp}(n)=15.72$] provided a value for the quantum efficiency $\eta(=0.098)$. Since μ_S is the known input, all parameters are determined and the theoretical curve can be drawn. The remainder of the experimental points are seen to cluster nicely about the theoretical curve.

Barlow, Levick, and Yoon used a 10-ms stimulus flash and a counting time $T=0.2$ s. The time course of their response showed that the ganglion-cell output in this interval could be roughly divided into two portions: a time $T_D \approx 130$ ms during which only spontaneous events appeared (with rate μ_D), and a time $T_S \approx 70$ ms during which the output was elevated (rate $\mu=\mu_S+\mu_D$). This is consistent with the results of Levick and Zacks [14]. The independence of the events in the two time slots permits us to compute the total mean and variance by simple addition. Although it might be thought that the nonstationary character of the light response at its edges could result in some error in our derivations, we have shown in prior work on the nonstationary SNDP that this is not the case [20].

The theoretical relationship between the variance and the mean (the solid curve around which the data lie) is characterized by a linear portion of slope ≈ 2.2 for sufficiently small mean. An initial slope larger than unity is a manifestation of multiplication noise. The effective multiplication parameter $\alpha_{eff} \approx 1.2$ is reduced from the value $\alpha=2$ assumed at the outset because of the presence of the refractoriness. At higher means the curve bends down. This is a more dramatic manifestation of the refractoriness which smoothes the noise and therefore reduces the variance. Without these two features of the model, multiplication and refractoriness, the data could not be fit as evidenced by the lower and upper dashed lines in Fig. 5. These represent results for the Poisson and best-fitting Neyman Type-A (NTA) distributions, respectively. Neither is in accord with the data.

Finally, in Fig. 6, we display the PND for Barlow, Levick, and Yoon's run No. 3 [$E_{exp}(n)=7.41$, $Var_{exp}(n)=15.72$]. The value of c is evidently sufficiently small ($c=0.918$) that the NTA theoretical distribution (solid curve) provides an adequate fit to the data as discussed in [18].

5 Conclusion

We have shown that the PID and PNDs for an on-center brisk-sustained retinal ganglion-cell at various (modest) levels of light stimulation can be understood in terms of a model containing four effects: Poisson quantum fluctuations, additive Poisson dark noise, Poisson multiplication noise (multiple neural spikes per absorbed photon), and refractoriness. All of these effects, including refractoriness, are important at all levels of light (including dark light alone). We believe that all four processes must be considered together to

understand the character of the neural point process in the retinal ganglion cell. Since the receiver operating characteristic (ROC) is constructed from the PNDs, it will also be fit by our model.

The parameters used to obtain the theoretical results were derived from the PID and two of the eight PNDs. They are physiologically plausible: a multiplication parameter $\alpha=2$, a characteristic impulse-response time $\tau_p=27\,\text{ms}$, a refractoriness time $\tau_d=1.7\,\text{ms}$, an equivalent dark photon rate $\mu_D=16.5\,\text{s}^{-1}$, and a quantum efficiency $\eta=0.098$. The latter turns out to be almost identical to the value obtained by Barlow, Levick, and Yoon for this unit ($\eta_{\text{BLY}}=0.097$) using the method of fixed-multiplicative-Poisson [7] sums. In some cases the quantity $c=\mu\tau_p$ is sufficiently small so that the PNDs are able to be fit by theoretical NTA distributions.

At low levels of illumination (near threshold) the statistical properties of the discharge are seen to behave like a multiplicative process with an effective multiplication parameter $\alpha_{\text{eff}}\approx 1.2$. The refractoriness is responsible for reducing the multiplication factor from 2 to 1.2. It is well known that the axons of the retinal ganglion cells comprising the optic nerve travel to central locations in the superior colliculus and lateral geniculate nucleus, and from there information is passed on to the primary visual cortex. Less well known, perhaps, are the results of recent measurements in single neurons of the cat and monkey visual cortex which demonstrate a proportionality of count variance to mean in that location as well [21–23]; this property is, of course, representative of a multiplicative process. We recall that randomly deleted [24] and/or cascaded [25] Poisson, Neyman Type-A (NTA), and shot-noise-driven Poisson (SNDP) counting distributions retain a variance-to-mean proportionality although the multiplication parameter is altered by these effects. From this study we have learned that at sufficiently low values of the mean, refractoriness operates on the point process in the same way. This leads us to observe that information carried up the visual pathway by a series of summations, deletions, and cascades retains the proportionality of variance to mean even in the presence of refractoriness. Such behavior provides justification for the good fit of multiplication-noise model predictions to Hecht-Shlaer-Pirenne experimental results [26, 27].

Finally, we note that changes in the spontaneous discharge level observed by Barlow, Levick, and Yoon during the course of their experiment can be understood quite well in terms of a simple change in the dark rate μ_D. This is because all data points collected during the course of their experiment lie near the universal theoretical curve for Unit BLF-1 with all parameters identical except μ_D.

Acknowledgements. This work was supported by the National Science Foundation. We wish to thank H. B. Barlow and W. R. Levick for providing us with the experimental data presented in Figs. 2, 5, and 6. We are particularly grateful to W. R. Levick for his careful description of the experimental apparatus and computer-output format.

References

1. Hecht, S., Shlaer, S., Pirenne, M.H.: Energy, quanta, and vision. J. Gen. Physiol. **25**, 819–840 (1942)
2. Barlow, H.B., Levick, W.R., Yoon, M.: Responses to single quanta of light in retinal ganglion cells of the cat. Vision Res. **11**, Suppl. 3, 87–101 (1971)
3. Levick, W.R.: Form and function of cat retinal ganglion cells. Nature **254**, 659–662 (1975)
4. Barlow, H.B.: Retinal noise and absolute threshold. J. Opt. Soc. Am. **46**, 634–639 (1956)
5. Levick, W.R., Thibos, L.N., Cohn, T.E., Catanzaro, D., Barlow, H.B.: Performance of cat retinal ganglion cells at low light levels. J. Gen. Physiol. **82**, 405–426 (1983)
6. McGill, W.J.: Poisson counting and detection in sensory systems. In: Concepts in communications: interpersonal, intrapersonal, and mathematical, Chap. 9, pp. 257–281, Beckenbach, E.F., Tompkins, C.B., eds. New York: Wiley 1971
7. Teich, M.C.: Role of the doubly stochastic Neyman Type-A and Thomas counting distributions in photon detection. Appl. Opt. **20**, 2457–2467 (1981)
8. Teich, M.C., Saleh, B.E.A.: Interevent-time statistics for shot-noise-driven self-exciting point processes in photon detection. J. Opt. Soc. Am. **71**, 771–776 (1981)
9. Saleh, B.E.A., Teich, M.C.: Multiplied-Poisson noise in pulse, particle, and photon detection. Proc. IEEE **70**, 229–245 (1982)
10. Baylor, D.A., Lamb, T.D., Yau, K.-W.: Responses of retinal rods to single photons. J. Physiol. **288**, 613–634 (1979)
11. Yau, K.-W., Matthews, G., Baylor, D.A.: Thermal activation of the visual transduction mechanism in retinal rods. Nature **279**, 785–786 (1979)
12. Baylor, D.A., Matthews, G., Yau, K.-W.: Two components of electrical dark noise in toad retinal rod outer segments. J. Physiol. **309**, 591–621 (1980)
13. Nunn, B.J., Baylor, D.A.: Visual transduction in retinal rods of the monkey *Macaca fascicularis*. Nature **299**, 726–728 (1982)
14. Levick, W.R., Zacks, J.L.: Responses of cat retinal ganglion cells to brief flashes of light. J. Physiol. **206**, 677–700 (1970)
15. Levick, W.R.: Personal communication
16. Mastebroek, H.A.K., Zaagman, W.H., Kuiper, J.W.: Intensity and structure of visually evoked neural activity: rivals in modeling a visual system. Vision Res. **17**, 29–35 (1977)
17. Teich, M.C., Khanna, S.M.: Pulse-number distribution for the neural spike train in the cat's auditory nerve. J. Acoust. Soc. Am. **77**, 1110–1128 (1985)
18. Saleh, B.E.A., Tavolacci, J.T., Teich, M.C.: Discrimination of shot-noise-driven Poisson processes by external dead time: Application to radioluminescence from glass. IEEE J. QE **17**, 2341–2350 (1981)
19. Teich, M.C., Diament, P.: Relative refractoriness in visual information processing. Biol. Cybern. **38**, 187–191 (1980)

20. Saleh, B.E.A., Teich, M.C.: Statistical properties of a non-stationary Neyman-Scott cluster process. IEEE Trans. IT **29**, 939–941 (1983)
21. Tolhurst, D.J., Movshon, J.A., Thompson, I.D.: The dependence of response amplitude and variance of cat visual cortical neurones on stimulus contrast. Exp. Brain Res. **41**, 414–419 (1981)
22. Dean, A.F.: The variability of discharge of simple cells in the cat striate cortex. Exp. Brain Res. **44**, 437–440 (1981)
23. Tolhurst, D.J., Movshon, J.A., Dean, A.F.: The statistical reliability of signals in single neurons in cat and monkey visual cortex. Vision Res. **23**, 775–785 (1983)
24. Teich, M.C., Saleh, B.E.A.: Effects of random deletion and additive noise on bunched and antibunched photon-counting statistics. Opt. Lett. **7**, 365–367 (1982)
25. Matsuo, K., Saleh, B.E.A., Teich, M.C.: Cascaded Poisson processes. J. Math. Phys. **23**, 2353–2364 (1982)
26. Teich, M.C., Prucnal, P.R., Vannucci, G., Breton, M.E., McGill, W.J.: Multiplication noise in the visual system at threshold: 1. Quantum fluctuations and minimum detectable energy. J. Opt. Soc. Am. **72**, 419–431 (1982)
27. Prucnal, P.R., Teich, M.C.: Multiplication noise in the human visual system at threshold: 2. Probit estimation of parameters. Biol. Cybern. **43**, 87–96 (1982)

Received: February 16, 1985

Professor B. Saleh
University of Wisconsin-Madison
Department of Electrical and
Computer Engineering
Madison, WI 53706
USA